Geologie und Paläontologie in Westfalen (2024): 3-14

An Early Pleistocene paleosinkhole in the Rhenish Massif, Germany

Mathias Knaak, Rüdiger Stritzke, Ulrike Wefels, Stefan Henscheid & Daniel Schrijver

Mathias Knaak
Geological Survey of Northrhine-Westphalia
De-Greiff-Str. 195
47803 Krefeld
Germany

Rüdiger Stritzke
Department of Earth Sciences
Ruhr-University Bochum
Universitätsstr. 150
44801 Bochum
Germany

Ulrike Wefels,
Stefan Henscheid &
Daniel Schrijver
Geological Survey of Northrhine-Westphalia
De-Greiff-Str. 195
47803 Krefeld
Germany

corresponding author:
ruediger.stritzke@rub.de

Manuskript
Eingegangen: 06.03.2024
Akzeptiert: 01.07.2024
Online verfügbar: 10.07.2024

Abstract

Karstification and development of caves and sinkholes are a common feature of Devonian reef limestone complexes in the Rhenish Massif. Sinkhole deposits formed shortly after reef emergence in the Devonian to the present day. These deposits are a remarkable archive of paleo-climate and paleo-environmental conditions.
Early Pleistocene clastic deposits have been exposed in a paleosinkhole during mining at the Düstertal quarry near Bleiwäsche/Brilon Reef Area. Comparable sedimentary sequences from this time period are scarce in northern and central Germany. Palynological and accompanying heavy mineral analysis imply that the described sedimentary sequence in the sinkhole deposits can be assigned to the Bavel Complex of the Early Pleistocene.

Keywords: Rhenish Massif; Germany; sinkhole; Early Pleistocene

Zusammenfassung

Verkarstung, Höhlenbildung und Dolinen sind weit verbreitete Phänomene in den devonischen Riffkomplexen des Rheinischen Massifs. Dolinenfüllungen bildeten sich kurz nach der Riffentstehung bis zum heutigen Tag. Diese Ablagerungen sind ein exzellentes Archiv der Paläoklima und -Umweltbedingungen.
Während Abbauarbeiten im Steinbruch Düstertal nahe Bleiwäsche/Briloner Riff erschlossen sich in einer Paläodoline frühpleistozäne klastische Ablagerungen. Vergleichbare Sedimentabfolgen aus dieser Periode sind selten in Nord- und Mitteldeutschland. Palynologische und beleitende Schwermineralanalysen implizieren, dass die beschriebene sedimentäre Dolinenfüllung in den Bavelkomplex des frühen Pleistozäns datiert.

Schlüsselwörter: Rheinische Masse; Deutschland; Karstschlotte; Frühpleistozän

Introduction

During mining at the Düstertal quarry near Bleiwäsche at the eastern edge of the Brilon Reef Complex/ Sauerland/Germany a paleosinkhole had been exposed (Fig.1). The aim of this contribution is to shed more light on the origin of this paleosinkhole filled with Early Pleistocene unconsolidated sediments.

The knowledge about the formation of karst in limestone deposits and its genesis is of great importance with regard to raw material exploration, hydrogeology, engineering geology and geothermal energy, but also for the assessment of geohazards.

Karstification requires soluble rocks, such as limestone, favorable climatic factors, and an appropriate hydraulic regime (White, 1988). Environmental changes cause fluctuations and even stagnation in karst development and thus the formation of paleokarst. In many cases, the development of sinkholes filled with clastic sediments is due to complex gravitational subsidence or collapse processes in karstified rocks. Gutiérrez et al. (2008) distinguish between slow subsidence of a cover sagging sinkhole (Subrosionssenke), e.g., due to solution processes at the boundary between karstified carbonates and overlying unconsolidated overburden (Lösungsdoline), and sudden collapse of a cover collapse sinkhole on top of a preexisting cavity in karstified carbonate (Erdfall resp. Einsturzdoline), depending on the process. For further definitions and terminological problems related to karst see Ahnert (1996), Ford & Williams (1989), Williams (2003) and Klimchouk (2017).

The Devonian reef limestone deposits of the Rhenish Massif are characterized by intensive karstification. Especially in the eastern Sauerland, numerous karst infill deposits within the Brilon reef limestone as well as adjacent reef limestone areas, such as the Warstein or the Hönne Valley area, have been known for a long time and partly investigated and described (e.g. Wirth 1964;

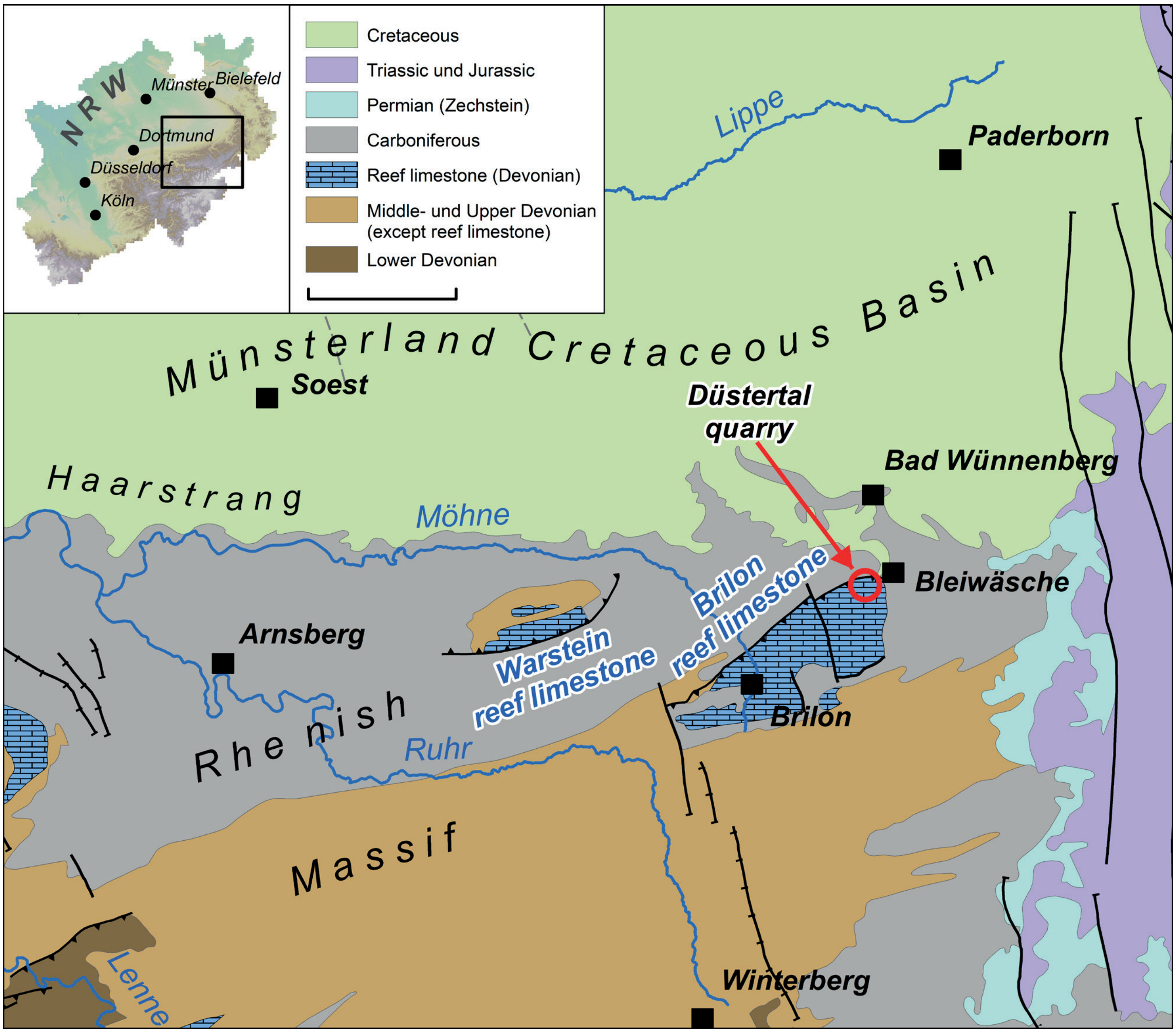

Fig. 1: Location of the Düstertal quarry (red circle) in the NE section of the Brilon reef limestone complex, eastern part of North Rhine-Westphalia (NRW); schematic geological overview after maps of the Geological Survey of North Rhine-Westphalia (GD NRW; scale bar: 5 km).

Meiburg 1979; Clausen 1979; Grebe 1982; Clausen & Leuteritz 1989; Ribbert & Skupin 2009). Different ages of karst infill deposits provide evidence for a long-lasting karstification development, which has been shown to extend at least from the Lower Cretaceous to the Pleistocene. Well-known examples in the Brilon reef limestone are karst infill deposits of Paleogene age of the Malachite Dome Cave (Arnold et al. 1992) and Lower Cretaceous-age karst infill deposits of Nehden (Grebe 1982). A very early onset of karstification is documented by pre-Variscan paleokarst cavity infill deposits formed shortly after deposition and diagenesis of the Devonian reef limestone (Bär 1966, 1968; Hagemann 1988).

The recent relief of the Brilon plateau is characterized by young morphological depressions, which were mainly caused by Pleistocene to recent karstification.

Middle to Upper Devonian reef carbonates of the Brilon reef limestone are mined in the Düstertal quarry near Bleiwäsche in the eastern Sauerland. The reef limestone here consists mainly of massive to moderately bedded, fine- to coarse-grained, light to dark gray limestone and locally cellular dolomite. Structurally, the quarry is located on the northern limb of the shallowly northeast plunging Brilon anticline formed during Variscan folding. Accordingly, the strata dip shallowly to moderately steeply to the NNE on average (dip direction/dip = 025/40°). Subsequently, Paleozoic rocks were dissected into fault blocks by NNW striking faults during syn- and post-Variscan, predominantly Mesozoic, deformation (e.g. in Ribbert et al. 2006).

Both near the surface and at greater depths, the limestone is partly intensively karstified along structural discontinuities such as fractures and small faults. The reef limestone of the Düstertal quarry is part of the Devonian Brilon reef limestone complex, which forms a karst area with dry valleys and sinkholes on the Brilon plateau (Zygowski 1983; Feige 1991).

In 1987, a cross-regionally important karst cave, the Malachite Dome, was discovered in the eastern part of the quarry (Erlemeyer et al. 1992) (Fig. 2). Therein cavities have been reliably proven to a depth of more than 80 m below surface. Age dating of the oldest cave sediments in the Malachite Dome indicate a Paleogene age of the sediments (Oligocene, Arnold et al. 1992). Dating of Weichselian speleothems provides evidence that karst development was still active during the last cold period (Richter et al. 2020), presumably continuing to the present. Cretaceous and other older sediments, as often evidenced in caves and karst infill deposits of the northern Sauerland (e.g., Clausen 1979; Huckriede 1982), are absent from the malachite dome. Therefore, phases of intensive karstification are attested for the area of the cave system of the Malachite Dome only from the Tertiary on. So far no carbonaceous sinkhole deposits are known here.

In 2018, progressive mining in the southwestern part of the Düstertal quarry exposed a sinkhole for a short period of time on the uppermost level (ca. 437 m NHN to the top of the terrain at ca. 448 m NHN) with a cut of ca. 50 m in width and ca. 9-11 m in height. The sinkhole was predominantly filled with fine-grained, dark gray, mostly clayey, carbonate-free, clastic unconsolidated sediments.

In the area of the reef limestone adjacent to the described dolina, two preferred fracture orientations

Fig. 2: Location of the described sinkhole and the Malachitdom cave in the Düstertal quarry (aerial photo data Geobasis NRW, 2023); red square marks the location of the map in figure 3 (scale bar: 1 km).

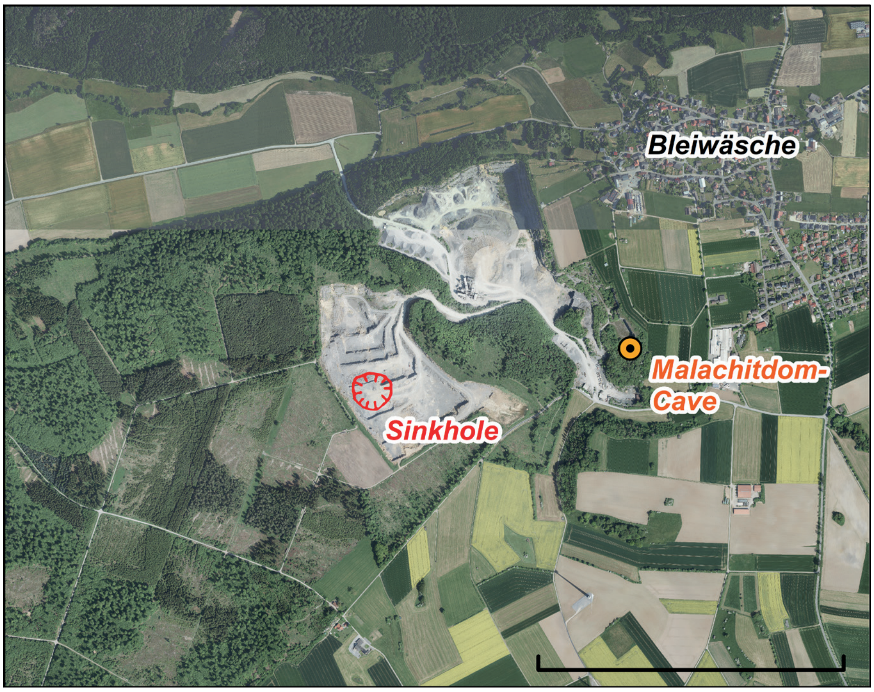

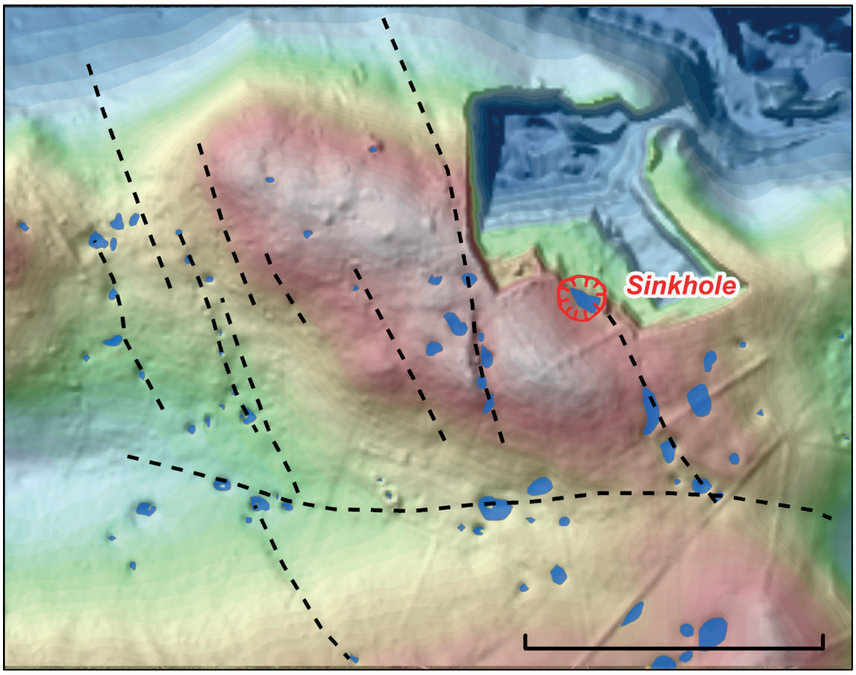

Fig. 3: Hillshade representation of the digital terrain model (Geobasis NRW, 2021) with the described sinkhole, colored according to altitude (warm colors = high areas, cold colors = lower areas) in the southwestern part of the Düstertal quarry. In the digital terrain model, a large number of drainless depressions can be identified to the southwest adjacent to the quarry, which are also interpreted as sinkholes (blue polygons). They occur preferentially along linear structures (dashed lines), which have the same orientation as the main fracture sets in the quarry (scale bar: 500 m).

were recorded within the quarry, with NNW (dip direction/ dip = 250/85°) and E striking (dip direction/ dip = 190/82°) fractures. The two fracture sets form an approximately orthogonal fracture system with steep, nearly vertical fracture surfaces. Similar directions are trailed by linear structures that can be mapped out along numerous sinkholes southwest of the quarry in the digital terrain model (Fig. 3).

Methodology

The quarry face of the approximately 10 m high uppermost bench was difficult to access for systematic sampling. Therefore, two small boreholes (11 m and 12.5 m deep; borehole numbers 315973 and 318922 in the database of the GD NRW) were sunk directly above the quarry face at the natural ground surface (approx. 446 m NHN) and within the karst infill deposits in order to obtain samples over the entire strata sequence of the sinkhole infill deposits.

From the 11 m deep small borehole 77 samples were analyzed palynologically. An additional 20 samples were collected to determine heavy mineral spectra from the 12.5 m deep borehole. Three individual samples from the quarry wall were examined micropaleozoologically.

Due to progressive quarrying the outcrop was accessible only for a short period of time. Therefore, a terrestrial laser scan was taken to accurately document the outcrop geometry (Figs. 3a and 3f) and photos were shot for a photogrammetric 3D reconstruction.

Lithological Sequence

The sequence of strata within the sinkhole is described below on the basis of observations at the quarry wall and the two small boreholes above the quarry wall from top to bottom. In the sinkhole, which is filled with unconsolidated sediments, mainly stiff carbonate-free gray clays to clayey silts are deposited under a thin cover of a loess derivative and humic topsoil. Peat layers up to decimeters thick are intercalated in the clays in the upper third. They divide the clayey sequence into an upper light gray clay and a lower darker clay. When wet, the lower clay has a predominantly blackish-gray color and is tough-plastic to stiff; when dry, the lower clay is mostly gray to light gray and hard, similar to the upper clay.

The clay is generally monotonous, but occasionally individual light gray layers up to a maximum of 5 cm thick occur, as well as sporadic intercalations of silty layers or occasional interlayered accumulations of sand and small boulder grains in thin layers, which indicate fine stratification. The boulders appear partly strongly decomposed, are predominantly light gray to white and strongly porous (so-called 'Hottensteine'). Rarely single glauconite grains could be observed. In addition to the peat layers, individual drift woods up to 15 cm long and occasional plant chaff occur within the entire clay.

The rather rare banding and the peat layers reveal a fine stratification. It is clear from this that the loose sediments are predominantly shallowly bedded or dip with a slight inclination towards the only slightly bowl-shaped center of the sinkhole where they increase in thickness. Based on the intensity values from the laser scan data, it can be seen that there are several peat layers that do not extend continuously over the entire sinkhole, but are partially unconformably cut off by overlying sediments (Pl.1). Based on dissections of the lighter bands and layers with coarser grains, an intensive small-scale fracturing with both small normal and reverse sense of movement is apparent

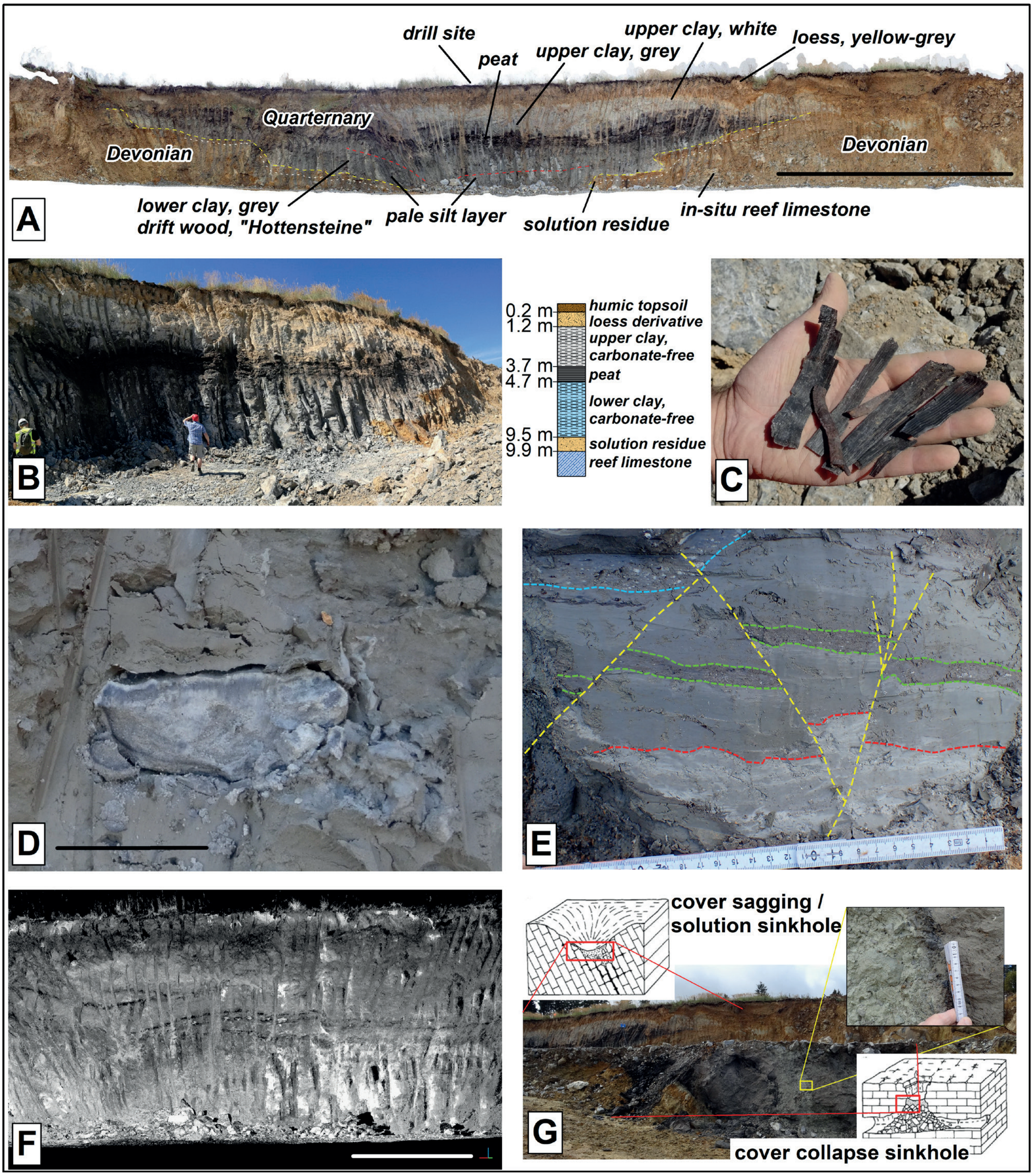

Fig. 4: **A** Side view of the photogrammetrically created digital outcrop model of the quarry wall (scale bar: 20 m). **B** Outcrop situation on 06th August 2018 and schematic lithological profile. **C** Drift wood pieces recovered from the clayey deposits of the sinkhole. **D** Friable "Hottenstein" within the clayey deposits (horizontal width of the "Hottenstein" is approximately 17 cm; scale bar: 10 cm). **E** Small-scale tectonics within the clayey deposits – lighter and partly somewhat coarser layers (blue, green and red dashed lines) illustrate the cm-scale offsets (yellow dashed lines represent faults). **F** Point cloud representation of the intensity values of the laser scan measurement - dark points represent a lower reflectivity e.g. organic rich layer. This clearly reveals structures that are not visible to the naked eye (scale bar: 5 m). **G** Oblique view of the upper part of the deeper excavation bench (foreground) showing chaotically bedded karst infill deposits and out of sequence and rotated reef limestone blocks in the area of a collapsed cavity (cover collapse sinkhole) and parts of the near-surface sediment-filled cover sagging/solution sinkhole in the upper quarry face (background); schematic sinkhole types after Ahnert (1996) and Ford & Williams (1989). Detailed view shows steeply dipping karst infill.

indicative of both local extensional and compressional regimes with dislocations at cm- to dm-scale.

This can be explained by the sagging of the sediment fill into an irregular funnel-shaped structure. To what extent these small-scale tectonics also affect the upper sedimentary parts of the sinkhole could not be clarified. A detailed recording of the geometry of the small-scale tectonics was not possible because of the consistency of the clay.

The lower part of the sinkhole and transition to the fractured reef limestone is formed by an approximately 0.2 to 1 m thick layer of light brown partially deconsolidated decalcified weathering residue of the reef limestone.

At the upper edge of the next deeper pit level, remains of a collapsed karst cavity were observed (Pl.1 G). Similar to the actual sinkhole described above, predominantly dark gray calcareous-free clays with low-thickness sandy to gravelly layers, bands and lenses occur there. However, these deposits are chaotic, partly steeply dipping to overturned, misaligned and mixed with large, partly decomposed reef limestone blocks and breccias. The extent to which the two deposits are related or should be considered independently could not be conclusively determined. However, the spatial location suggests that the lower chaotic part a of the lower quarry wall offers a glimpse into a deeper section of the same karst structure.

Heavy Mineral Analysis

Heavy mineral samples were generally taken at intervals of about 50 cm between 2 m and 12.3 m of a 12.5 m deep percussion drill hole (hole number 318922 in the GD NRW database). In figure 5, the red lines indicate the sampling depths. The heavy mineral distribution of the 20 present heavy mineral analyses show characteristic variations and can thus be subdivided into four different sections from stratigraphically youngest to stratigraphically oldest or from top to bottom.

The uppermost section down to 1.4 m depth clearly shows a Quaternary spectrum characteristic of late Pleistocene loess. Low contents of stable heavy minerals (zircon, tourmaline, rutile; together about 25%) are accompanied by increased contents of epidote and a from top to bottom decreasing content of green hornblende (30-14.5%). At the same time, individual volcanogenic minerals (clinopyroxene, brown hornblende and titanite) occur. This is in agreement with the site findings of a late Pleistocene loess-dominated solifluction soil.

Downhole this is followed by the upper clay, a section with very high contents of stable minerals of up to 96.5%. This may indicate a strong weathering, in which the proportion of stable heavy minerals is relatively increased. Possibly this also indicates mixing with redeposited Cretaceous sediments, in which the proportions of stable heavy minerals are basically increased. Since Cretaceous strata were eroded in the immediate vicinity of the sinkhole at the time of sedimentation (Ribbert et al. 2006), a combination of both is very likely.

From the depth range between 4.1 and 6.0 m no samples are available from which heavy minerals could be extracted to a sufficient extent. Here, however, a very strong change in the heavy mineral spectrum seems to occur.

In the underlying section up to about 10 m, the contents of stable minerals decrease to values around 50%. This range corresponds to the lower clay observed in the quarry wall.

From a depth of 10.5 m, an area with even lower contents of stable heavy minerals with values around 40 % and a simultaneous increase in the relative epidote content follows. Garnet is also partly more strongly represented in this section than in the upper part of the drill hole. Lithologically this section of the borehole is characterized by a higher proportion of somewhat coarser material such as silt and, in part, minor sand and gravel.

The variation of the proportions of individual heavy minerals in the karst infill deposit can be explained on the one hand by the different decomposition of the heavy minerals as a result of climatic variations, on the other hand it can be attributed to a different proportion of detrital input from slightly different supply areas during the deposition of this profile. Due to the lack of comparative results from this area, the heavy minerals alone do not allow a clear stratigraphic classification of the karst fill at present.

Micropaleozoological Results

Micropaleontological investigations were carried out on three samples from the quarry wall. In all three samples small amounts of Cretaceous marine nannoplankton (from Lower Cenomanian onwards) could be detected. Presumably, these are detrital alluvial deposits of Cretaceous material that were eroded in the near vicinity and transported into the sinkhole. Outcropping relics of Lower Cenomanian occur less than 1 km away (Ribbert et al. 2006).

Palynology

Palynological samples were collected at intervals of about 10 cm from an 11 m deep percussion drill hole (hole number 315973 in the GD NRW database). A total of 77 pollen samples were analyzed. After pretreatment with potassium hydroxide, the samples were subjected to hydrogen fluoride treatment (40%) followed by ultrasonic sieving (mesh size 6 x 8 µm) and final acetolysis according to Erdtmann (1952, 1960). The basis for the representation in the pollen diagram is the total pollen sum calculated from the amounts of woody and herbaceous plants = 100%. The pollen diagram (Fig. 6) was created using the software Tilia (Grimm 1991). Pollen counts of at least 100 to 300 were obtained for all of the present 77 palynologically studied samples. Therefore, a representation of the pollen sums in the pollen diagram was omitted.

Fig. 5: Synoptic comparison of lithology (drillhole BNUM 318922), view of quarry face as profile column (taken from laser scan) and heavy mineral distribution (drillhole BNUM 318922). Red lines indicate the sampling depths.

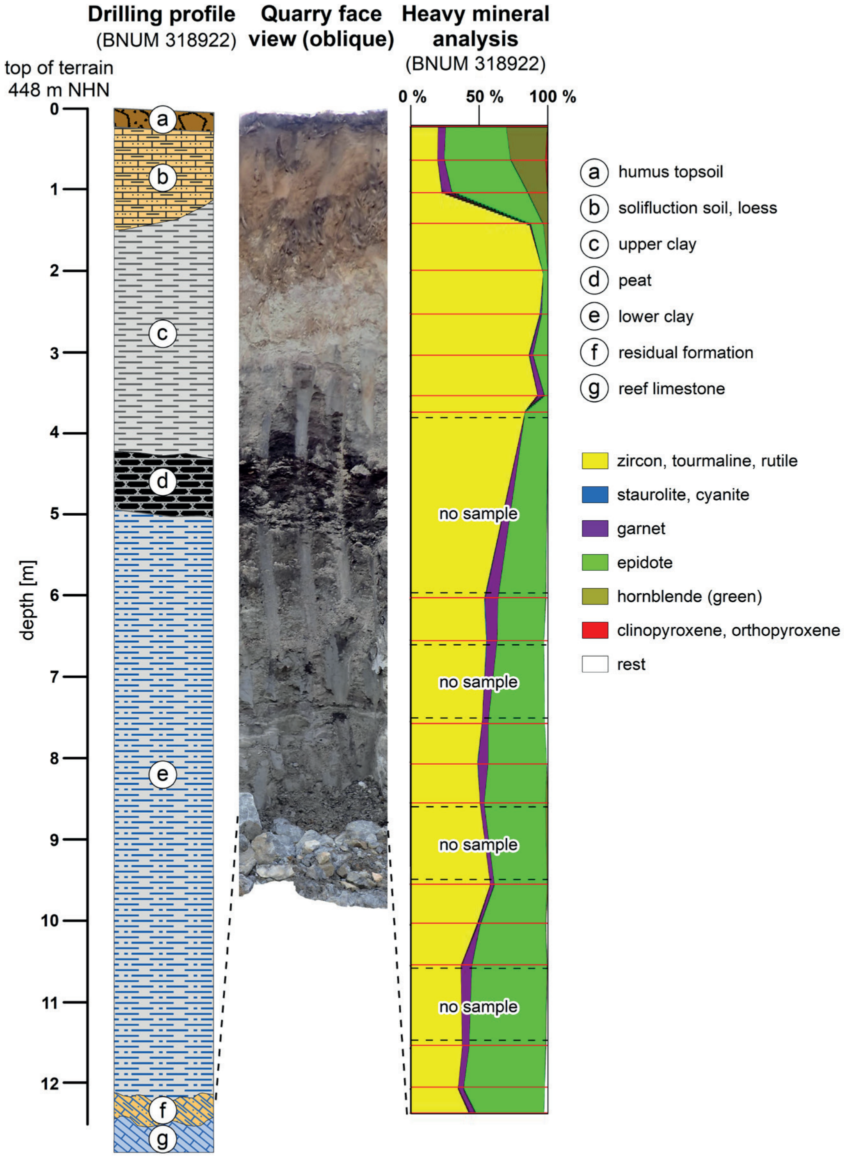

Vegetation history

The pollen distribution enables a zonal division into 10 LPAZ (local pollen assemblage zones; Blei I to Blei X, Fig. 6). Hereinafter the zones are described differing from the descriptions of the stratigraphic sequence and the distribution of the heavy minerals from bottom to top:

1. LPAZ I (Blei I): *Pinus*-Poaceae-*Picea* (-*Betula*) zone (8.50–9.45 m).

The pollen record starts with high pine (*Pinus*) and spruce (*Picea*) dominance. Associated are birch (*Betula*) trees. Coeval high grass values attest to an overall semi-open boreal coniferous forest commonly found in Pleistocene profiles. The proportion of other non-arboreal pollen (NAP) is also high. Mixed oak forest (MOF) is represented only by single pollen grains, especially those of elm (*Ulmus*). The transition to LPAZ II is marked by a significant decrease of *Picea* and *Betula* and an increase of mugwort (*Artemisia*).

2. LPAZ II (Blei II): Poaceae-*Pinus*-*Artemisia*-Ericales zone (8.35–8.50 m).

Herbaceous plants dominate this short zone. High rates of Poaceae, *Artemisia* and especially Ericales document a largely open cold steppe with subordinate woody plants. Only pine remains in higher rates. The transition to LPAZ III is marked by anewed increases in pine, spruce and birch with simultaneous decrease in Poaceae, *Artemisia* and Ericales.

3. LPAZ III (Blei III): Poaceae-*Betula*-*Artemisia* (-*Picea*) zone (6.40–8.35 m).

The increase in woody plants with simultaneously increasing rates of non-arboreal pollen (NAP) documents a semi-open cold steppe with increasing forest cover. Larch/Douglas fir (*Larix*) can be detected for the first time. The willow (*Salix*) curve is continuous on a low level. The transition to the overlying LPAZ IV is characterized by a significant decrease in NAP, especially grasses

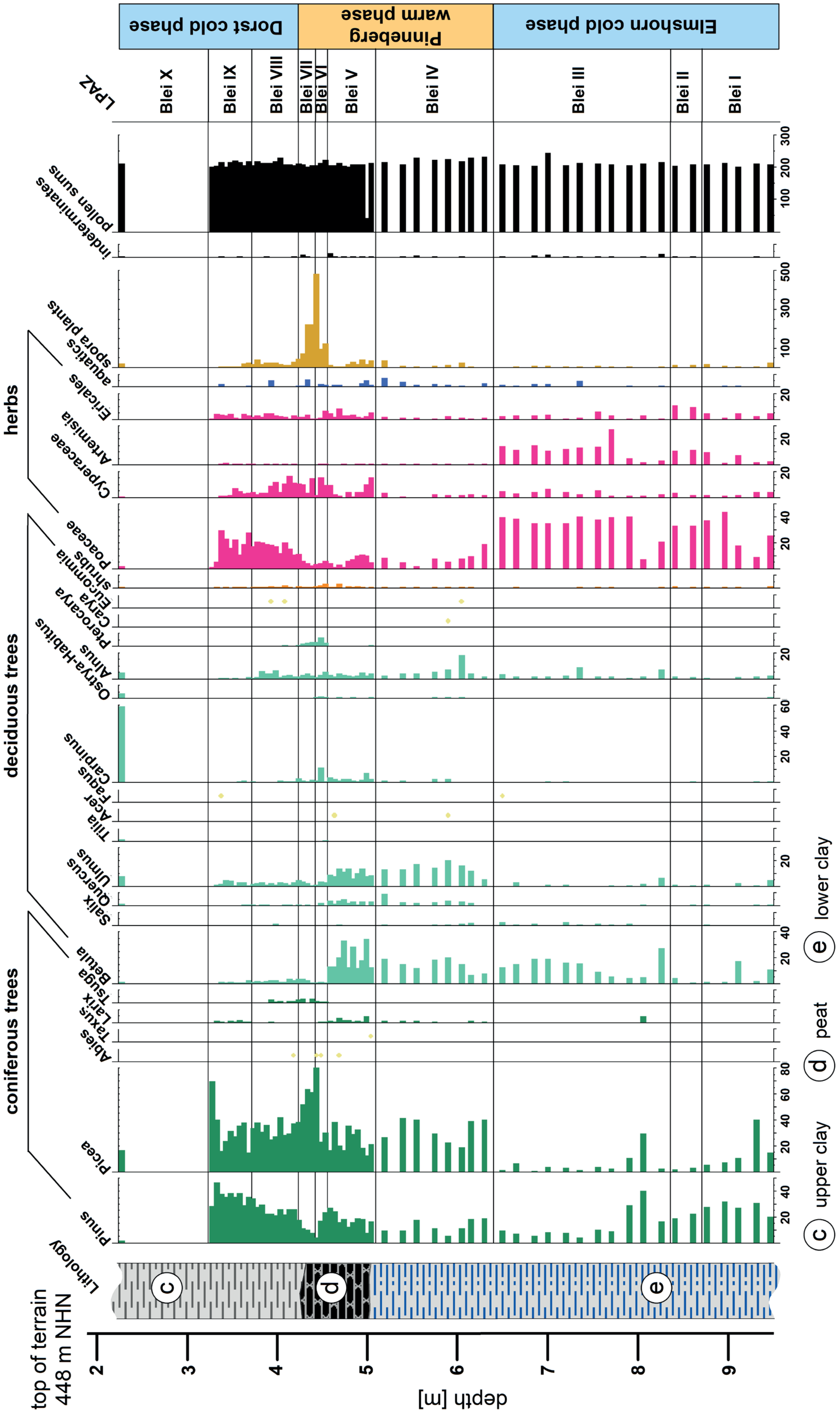
Dorst cold phase
Pinneberg warm phase
Elmshorn cold phase
LPAZ
Blei X
Blei IX
Blei VIII
Blei VII
Blei VI
Blei V
Blei IV
Blei III
Blei II
Blei I
pollen sums
indeterminates
spora plants
aquatics
Ericales
Artemisia
Cyperaceae
Poaceae
shrubs
Eucommia
Carya
Pterocarya
Alnus
Ostrya-Habitus
Carpinus
Fagus
Acer
Tilia
Ulmus
Quercus
Salix
Betula
Tsuga
Larix
Taxus
Abies
Picea
Pinus
Lithology
herbs
deciduous trees
coniferous trees
top of terrain 448 m NHN
depth [m]
2
3
4
5
6
7
8
9
100
200
300
500
20
40
60
80
c upper clay
d peat
e lower clay

and mugwort, with a simultaneous increase in spruce and mixed oak forest (MOF).

4. LPAZ IV (Blei IV): *Picea-Betula*-MOF zone (5.10–6.40 m).

LPAZ IV and V mark the thermal optimum in this profile. With increasing spruce and birch pollen rates the mixed oak forest (MOF) is clearly represented. In addition to oak, elm is the main species detected making up to 20% of the total pollen sum. The MOF seems to be complete with the proof of maple (*Acer*), linden (*Tilia*) and hornbeam (*Carpinus*). Hop hornbeam (*Ostrya*), wingnut (*Pterocarya*), hickory (*Carya*), and gutta-percha (*Eucommia*) are documented for the first time. The transition to LPAZ V is characterized by a slight decrease in oak (*Quercus*) and elm, and an increase in larch/Douglas fir and birch.

5. LPAZ V (Blei V): *Picea-Betula-Pinus*-MOF zone (4.57–5.10 m).

This zone is dominated by conifers and birch, but thermophilic woody plants are noticeably represented in mostly continuous curves. Oak and especially elm dominate in the mixed oak forest which contained also lime, maple and hornbeam. Hop hornbeam can be found repeatedly. Fir (*Abies*), yew (*Taxus*), hemlock (*Tsuga*), juniper (*Juniperus*) and especially larch are found in continuous curves. The boundary to LPAZ VI is marked by a significant drop of birch and elm and the beginning of a continuous curve of winged walnut and larch.

6. LPAZ VI (Blei VI): *Picea* (-*Pinus*-Poaceae-Cyperaceae) zone (4.43–4.57 m).

This zone is characterized by very high spruce values (77%). Rising pine and grass ratios provide evidence of increased cooling. Consequently, MOF values are decreasing. The continuous oak curve ends here. The elm curve also drops significantly, but remains closed. Linden and hop hornbeam are sporadically proven. Hornbeam shows an intermediate maximum (24%), as does wingnut (14%). Fir and larch are sporadically detected. The continuous curve of hemlock starts with low values (about 3%). The transition to the following LPAZ VII is characterized by a decline of spruce, the exposure of larch, the decline of hornbeam and the end of hop hornbeam.

7. LPAZ VII (Blei VII): *Picea*-Cyperaceae (-Poaceae) zone (4.25–4.43 m).

Spruce still dominates the vegetation but declines. Reed (Cyperaceae) and above all sweet grasses (Poaceae) are increasingly significant progressivley climatic cooling. Thermophilic elements are scarce. The MOF is represented only by elm and hornbeam. Oak is only represented by isolated pollen grains. Wingnut is also declining, its curve remaining continuous on a low level. Hemlock pollen remain. The transition to LPAZ VIII is marked by a further decrease of spruce and a clear increase of pine and especially of sweet grasses.

8. LPAZ VIII (Blei VIII): *Pinus-Picea*-Poaceae (-Cyperaceae) zone (3.73–4.25 m).

Pine and spruce are the dominant woody plants and grasses are the dominant herbs in this zone. This represents a semi-open boreal coniferous forest. Thermophilic elements are scare with only elm showing a continuous curve on low level (appr. 6%). The continuous curve of Alder (*Alnus*), wingnut and hemlock end in this zone. Fir and gutta-percha are sporadically proven. The transition to LPAZ IX is marked by decreasing spruce and increasing pine rates, the termination of hemlock as well as alder and birch.

9. LPAZ IX (Blei IX): *Pinus-Picea*-Poaceae zone (3.30–3.73 m).

Pine and spruce are the dominant woody species. Poaceae rates are high. This zone again represents a semi-open boreal coniferous forest like LPAZ VIII with all woody species except Pine and elm are present only sporadically. Worth mentioning is a nearly closed larch curve at a low level (appr. 3%). The zone ends at a hiatus at 3.30 m.

10. LPAZ X (Blei X): *Carpinus-Picea* (-*Ulmus*) zone (2.20 m).

Only one sample represents this zone. The hornbeam is the dominant

woody plant (60%). Also spruce (15%) and elm (7%) are clearly represented. Pine, birch,

oak, linden and alder are proven at low rates (<5%).

Stratigraphic Position

A classification of the karst stratigraphic sequence into the Eemian or Holstein Warm Period can be discarded because of the completely different vegetation development. In the Cromer complex *Eucommia* is found, but not *Ostrya* (Zagwijn & Zonneveld 1956; Grüger 1967). Since hemlock (*Tsuga*) can be traced in the sinkhole deposits up to the upper parts of the profile, the succession belongs to the Early Pleistocene rarely known in Central Europe. Zagwijn (1992) presented a summary of the Early Pleistocene palynostratigraphy. A more recent

Fig. 6 (opposite side): Pollen diagram (drillhole BNUM 315973) including local pollen assemblage zones (LPAZ) and their stratigraphic assignment in cold and warm periods within the Bavel Complex (1,030,000 - 850,000 yrs.).

summary was published by Litt et al. (2007). Accordingly, the described sequence does not fit into the Tegelen or the Waal complex. This is because these interglacial complexes differ from the younger interglacials in lacking distinguishable immigration sequences of forest trees (Zagwijn 1963).

In contrast, those immigration sequences are known since the Bavel Complex interglacials. Something like that can also be identified in the sinkhole profile described here. After an initial phase (Blei I-III) an immigration of thermophilic woody plants is clearly recognizable in zones IV and V. Since a classification into the Cromer complex can be excluded (see above), the entire presented sequence up to the uppermost zone Blei X dates into the Bavel complex (1,030,000 - 850,000 years ago). Menke (1969) was able to examine this complex in more detail in the deposits from Lieth near Elmshorn. He subdivides the Bavel complex (from bottom to top) into an Uetersen warm period, an Elmshorn cold period, a Pinneberg warm period and a final Dorst cold period. The difference between the Uetersen-Warm Period and the Pinneberg-Warm Period is that in the latter neither hornbeam (*Carpinus*) nor hemlock (*Tsuga*) are represented in appreciable proportions. This is likewise the case in the present sinkhole profile. The *Ulmus* peak described in the Pinneberg Warm Period is also present here in the Blei IV zone.

Consequently, the sedimentary sequence in the karst deposits at Bleiwäsche can be assigned to the Elmshorn Cold Period (Zones I - III), the Pinneberg Warm Period (Zones IV-VII) and the Dorst Cold Period (Zones VIII, IX) of the Bavel Complex. The vegetation signal of zone X cannot be assigned palynostratigraphically; it is atypical and, moreover, hardly documented with only one sample. The high *Carpinus* values might point to the Cromer complex.

Conclusions

The palynological evaluation of the samples indicates a Quaternary age (Lower Pleistocene, Bavel Complex).

The examination of the heavy minerals does not allow a clear stratigraphic assignment due to the lack of comparative examinations, but does not contradict the palynological results.

The present investigations confirm a predominantly Early Pleistocene formation period of the solution doline, which subsided and filled with clastic deposits over a longer period during two cold and one intervening warm period of the Bavel Complex. The bowl-shaped sinkhole sediments are homogenous, finely banded and dip only weakly towards the lowest point of the depression (Fig. 7).

The solution of the underlying carbonates of the Brilon reef limestone occurred at the contact between the Quaternary unconsolidated sediments and the Devonian carbonates. Therefore, one can use the terminology of a covered karst and a solution dolina. Solution residues formed at the transition between the carbonates and the fine clastic unconsolidated sediments. The largely insoluble and low-permeability Quaternary-aged deposits continuously subsided due to the long-lasting karstification process, as evidenced by intense small-scale tectonics within the unconsolidated sediments. Broughton (2017) describes similar phenomena associated with evaporite karst and the sometimes-rapid vertical subsidence of overlying unconsolidated sediments including fragmentation of sediments and both compressive and extensional fracture-like deformation phenomena.

Overall, this type of karstification takes place slowly through long-lasting processes. The most complete sequence is therefore located in the central area of the karst structure.

The thin cover of the sinkhole deposits by presumably Weichselian loess or its derivatives, which seem to be largely unaffected by the karst processes, indicates that the solution process within the solution dolina described here was at least largely completed pre- Weichselian and subsequently continued at most very slightly.

The comparably composed, but highly dislocated and chaotic Quaternary karst infill deposits observed at a nearby lower bench of the quarry (fig. 4 G), suggest that pre-existing cavities in the reef limestone (the age of the cavities is uncertain) collapsed during or after the Bavel Complex by a rather sudden event. The slow, long-lasting solution processes of the near-surface dolina, the cave formation within the reef limestone (partly at greater depths) and the collapse of pre-existing cavities are therefore to be regarded as temporally and genetically separated processes. Presumably, the processes that led to the formation of the solution dolinas occur more frequently where the reef limestone is already predisposed by faults or intensive fracturing and where karstification already took place linearly or caused cavities towards depth at earlier stages. This is also supported by the linear arrangement of further sinkholes in adjacent areas. The formation of caves in the area of the Düstertal quarry, such as the Malachite Dome Cave, took place at a different time and under different conditions than the formation of the solution dolina described here. Thus, the herein described sinkhole is evidence of intensive and long-lasting near-surface karstification during the Early Pleistocene of the Quaternary. Since evidence of Early Pleistocene

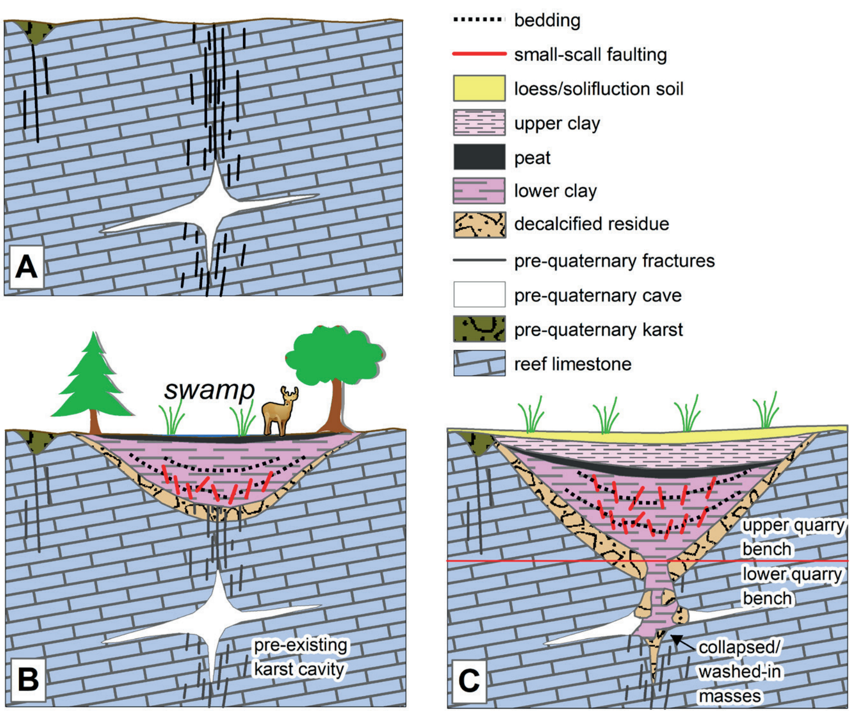

Fig. 7: Schematic development of near-surface epikarst comprising a covered Quaternary solution sinkhole above a karst cave system. **A** Pre-Quaternary cave and karst infill development along pre-existing fracture systems (Paleogene/Neogene cave, e.g. Malachitdom). **B** Syn-Early Pleistocene covered karst including development of a cover sagging sinkhole caused by the dissolution of limestone at the limestone-karst infill interface at the base of the sinkhole. **C** Today, Weichselian loess overlays the advanced cover sagging sinkhole accompanied by intensive small-scale tectonics of the insoluble fine-grained clastic deposits during long-lasting solution and sagging, and collapse of pre-existing cave systems.

processes and resulting sedimentary deposits has been rare and therefore little studied, the sinkhole described here and the sediments trapped within it are of particular importance.

Acknowledgements

We would like to thank Andreas Schudelski for pointing out the outcropping sinkhole. Furthermore we would like to acknowledge the Sauerländer Hartkalkstein-Industrie GmbH for the opportunity to investigate the sinkhole and the drilling team of the GD NRW for their efforts in drilling the percussion drill holes. We thank Dr. Philipp Stojakowits (Landesamt für Bergbau, Energie und Geologie Niedersachsen) for critically revising the manuscript and Dr. Jürgen Hahne (University of Göttingen) for revising the palynostratigraphic section.

References

Ahnert, F. 1996: Einführung in die Geomorphologie. Ulmer Press: Stuttgart.

Arnold, G., Burger, D., Erdelbrock, K., Schmidt, K.-H., Stritzke, R., Thomas, L., Vieth-Redemann, A., Wrede, V., Wurl, J. & Zehmke, E. 1992. Sedimentuntersuchungen im Malachitdom. In: Geologisches Landesamt Nordrhein-Westfalen (ed.). Der Malachitdom: Ein Beispiel interdisziplinärer Höhlenforschung im Sauerland, 205-236. Krefeld.

Bär, P. 1966. Stratigraphie, Fazies und Tektonik am Briloner Massenkalk-Sattel (Ostsauerland). – PhD Thesis, University Gießen.

Bär, P. 1968. Die ober-devonisch/unter-karbonische Schichtlücke über dem Massenkalk des Briloner und Messinghäuser Sattels (Ost-Sauerland). – Neues Jahrbuch für Geologie und Paläontologie - Abhandlungen 131: 263–288.

Broughton, P. 2017. Hypogene karst collapse of Devonian Prairie Evaporite basin in Western Canada. In: Klimchouk A., N. Palmer A., De Waele J., S. Auler A., Audra P. (eds.). Hypogene Karst Regions and Caves of the World. Cave and Karst Systems of the World. 617-632. Cham: Springer.

Clausen, C.-D. 1979. Über kreidezeitliche bis pleistozäne Karstfüllungen im Warsteiner Massenkalk (Rheinisches Schiefergebirge). – Aufschluss, Special Edition 29: 113-124.

Clausen, C.-D. & Leuteritz, K., mit einem Beitrag von Rescher, K. & Leuteritz, K. 1989. Spalten und ihre Füllungen in den Carbonatgesteinen des Warsteiner Raumes (nordöstliches Rheinisches Schiefergebirge). – Fortschritte in der Geologie von Rheinland und Westfalen. 35: 309-391.

Erdtmann, G. 1952. Pollen morphology and Plant Taxonomy (An introduction to Palynology-1, Angiosperm). Stockholm: Almqvist and Wiksell.

Erdtmann, G. 1960. The acetolysis method, revised description. – Svensk Botanisk Tidskrift 54: 561-564.

Erlemeyer, M., Hasenmayer, B. & Schudelski, A. 1992. Das Höhlensystem Kreiselhalle-Malachitdom - Ein bemerkenswerter Aufschluss für Höhlenminerale. In: Geologisches Landesamt Nordrhein-Westfalen (ed.). Der Malachitdom: Ein Beispiel interdisziplinärer Höhlenforschung im Sauerland, 69-89. Krefeld.

Feige, W. 1991. Karstgebiete in Südostwestfalen und ihr Formenschatz. Geographische Kommission für Westfalen, 25-41. Münster.

Ford, D.C. & Williams, P. 1989. Karst Geomorphology and Hydrology. London: Chapman & Hall.

Grebe, H. 1982. Die unterkretazische Karsthöhlen-Füllung von Nehden im Sauerland. 2. Die Mikrosporen-Assoziationen, Altersaussage und Versuch eines Vegetationsbildes. – Geologica et Palaeontologica 16**:** 243-258.

Grimm, E.C. 1991. TILIA and TILIA·GRAPH computer programs. Illinois State Museum: Springfield.

Grüger, E. 1967. Vegetationsgeschichtliche Untersuchungen an comerzeitlichen Ablagerungen im nördlichen Randgebiet der deutschen Mittelgebirge. – Eiszeitalter und Gegenwart – Quaternary Science Journal 18: 204–235.

Gutiérrez, F, Guerrero, J. & Lucha, P. 2008. A genetic classification of sinkholes illustrated from evaporite paleokarst exposures in Spain. – Environmental Geology 53: 993-1006.

Hagemann, P. 1988. Die Geologie des Gebietes N′ und W′ von Brilon/HSK. – Unveröffentlichte Diplomkartierung Ruhr-Universität Bochum, Bochum, Germany.

Huckriede, R. 1982. Die unterkretazischen Karsthöhlen-Füllung von Nehden im Sauerland. 1. Geologische, paläontologische und paläobotanische Befunde und Datierung. – Geologica et Palaeontologica 16**:** 183-242.

Klimchouk, A. 2017. Types and settings of hypogene karst. In: Klimchouk, A. et al. (eds.) Hypogene Karst Regions and Caves of the World. Cave and Karst Systems of the World, 1-39. Cham: Springer.

Lanser, K. P. 2015. Nachweis von Pterosauriern aus einer unterkreidezeitlichen Karstfüllung im nördlichen Sauerland (Rheinisches Schiefergebirge, Deutschland). – Geologie und Paläontologie in Westfalen 87: 93-117.

Litt, T., Behrke, K.-E. Meyer, K.-D., Stephan, H.-J. & Wansa, S. 2007. Stratigraphische Begriffe für das Quartär des norddeutschen Vereisungsgebietes. – Eiszeitalter und Gegenwart - Quaternary Science Journal 56: 7–65.

Meiburg, P. 1979. Die Höhlen im Warsteiner Massenkalk. – Aufschluss, Special Edition 29: 143-178.

Menke B. 1969. Vegetationsgeschichtliche Untersuchungen an altpleistozänen Ablagerungen aus Lieth und Elmshorn. – Eiszeitalter und Gegenwart - Quarternary Science Journal 20: 76–83.

Norman, D. B. & Hilpert, K.-H., mit einem Beitrag von Hölder, H. 1987. Die Wirbeltierfauna von Nehden (Sauerland), Westdeutschland. – Geologie und Paläontologie in Westfalen 8: 1-77.

Ribbert, K.-H., Skupin, K. & Oesterreich, B., mit Beiträgen von Farrenschon, J., Krahn, L., Nieskens, H. G., Pahlke, U., Roth, R. & Wrede, V. 2006. Geologische Karte von Nordrhein-Westfalen 1: 25 000, Erläuterungen zu Blatt 4518 Madfeld. 2., völlig neu bearbeitete Auflage. Krefeld.

Ribbert, K.-H. & Skupin, K. 2009. Marine und terrestrische Sedimente der Kreide-Zeit im Paläokarst des Briloner Massenkalks. – Geologie und Paläontologie in Westfalen 72: 71-92.

Richter, D. K., Schudelski, A., Neuser, R. D. & Scholz, D. 2020. Weichselzeitliche Umbrellacalcite aus der Höhle „Malachitdom“ (NE-Sauerland): vom Kaltwasser- zum Ausfrierstadium in Pools auf Eis. – Geologie und Paläontologie in Westfalen 94: 1-14.

White, W.B. 1988. Geomorphology and Hydrology of Karst Terrains. New York: Oxford University Press.

Williams, P. 2003. Dolines In: Gunn, J. (ed.). Encyclopedia of caves and karst science, 304-310. Oxfordshire: Routledge.

Wirth, W. 1964. Über zwei Unterkreiderelikte im nördlichen Sauerland. – Fortschritte in der Geologie von Rheinland und Westfalen 7: 403-420.

Zagwijn, W.H. 1963. Pollen-analytical investigations in the Tiglian of the Netherlands. – Mededelingen van de Geologische Stichting., Nieuwe Serie 16: 49–71.

Zagwijn 1992. The beginning of the Ice Age in Europe and its major subdivisions. – Quaternary Science Reviews 11: 583–591.

Zagwijn, W.H & Zonneveld J.I.S. 1956. The Interglacial of Westerhoven. – Geologie en Mijnbouw 18: 37–46.

Zygowski, D. 1983. Die Höhlen der Briloner Hochfläche (östliches Rheinisches Schiefergebirge). – Karst und Höhle 1982/83: 15-46